Research Article

Ying Zhang, Yangchen Fu, Qingguo Mao, Guohua Zhang*, Wenchao Zhang, Yi Wang, and Wenlong Yang

First-principle calculation of electronic structure and optical properties of (P, Ga, P–Ga) doped graphene

https://doi.org/10.1515/phys-2022-0061
received April 08, 2022; accepted June 21, 2022

Abstract: First-principle calculations are used to study the electronic structures, electronic and optical properties of pure, phosphorus-doped, aluminum-doped, and phosphorus and aluminum co-doped graphene. The gap between the conduction band and valence band of intrinsic graphene is zero. However, when graphene is doped with P, Ga, and P–Ga, the gap in energy will be opened and to a different extent. In the three different doping results, the gap values between the conduction and valence bands of P, Ga, and P–Ga graphene are 0.11, 0.35, and 0.39 eV, respectively. When graphene is doped with P–Ga, more electrons (1.40 e) will be gained by carbon atoms compared to P-doped graphene (0.61 e), while fewer electrons (1.49 e) will be transferred to carbon atoms compared to Ga-doped graphene (1.75 e). After doping with P, Ga, and P–Ga, the overall intensity of the graphene absorption peak is weakened and more pronounced relative to the low-frequency peaks. This result can fully demonstrate that the band gap of the doped graphene system can be better tuned by adding phosphorus and gallium atoms.

Keywords: graphene, co-doped, electronic structure, optical property, first-principle

*** Corresponding author: Guohua Zhang,** Jinhua Advanced Research Institute, Jinhua 321013, China, e-mail: ghzhang1982@sina.com
Ying Zhang: Jinhua Advanced Research Institute, Jinhua 321013, China
Yangchen Fu, Wenchao Zhang: School of Electrical and Electronic Engineering, Harbin University of Science and Technology, Harbin 150080, China
Qingguo Mao: Sanya Institute of Technology, Sanya 572022, China
Yi Wang: School of Physics, Harbin Institute of Technology, Harbin 150001, China
Wenlong Yang: School of Measurement and Control Technology and Communication Engineering, Harbin University of Science and Technology, Harbin 150001, China

1 Introduction

Scientists have been working with graphene since the early 1900s. However, stable graphene structures have not been obtained in experiments, until 2004, and the successful preparation of intrinsic graphene has led to a booming period of research on two-dimensional materials [1–4]. After this, the hot spot for basic science and advanced technology research has shifted to unique two-dimensional materials represented by graphene. Graphene has excellent properties in terms of light and electricity, force, and heat [5,6].

Graphene has excellent mechanical properties in the field of mechanics, such as Young's modulus, shear elasticity, and tensile strength, so its application prospects are very bright [7]. Moreover, graphene has extraordinary conductivity, flexibility, and optical transparency, and can be used as a transparent conductive film material in solar cells and light-emitting diodes [8] The light modulator made of graphene has a strong signal transmission capability, which can transmit a large amount of information and data in a short time [9]. In the field of electronic devices, graphene is considered to be one of the most potential electronic device materials in the post-silicon era, and is expected to become a new cornerstone in the field of microelectronics [10]. Ultra-high carrier mobility and micron-level ballistic transmission characteristics make graphene-based electronic and optoelectronic devices have ultra-high-speed frequency response characteristics [11,12]. Graphene lithium battery cathode material is wrapped with graphene as a conductive paste, which can improve the conductivity of the electrode, increase the rate performance of the battery, and increase the cycle stability [13,14]. The graphene lithium battery with graphene as the negative electrode has high capacity and fast charging speed [15,16]. Graphene supercapacitors have high electrochemical performance and higher specific surface area, have ultra-fast charge and discharge

performance, better ductility, and longer life [17–20]. Graphene also shows good performance in the application of field-effect transistors and radio frequency transistors [21]. Graphene-based flexible transistors have good flexibility and temperature stability, and can work at room temperature. The excellent physical and chemical properties of intrinsic graphene make it have potential and broad application prospects in many fields [22] However, the high carrier mobility but low carrier concentration of intrinsic graphene greatly limits the application of intrinsic graphene in digital circuits. In addition, intrinsic graphene has limited adsorption capacity for heterogeneous atoms or molecules [23]. In order to better realize the application of graphene in many directions, it is necessary to modify graphene. The introduction of foreign elements into graphene can control the electronic properties of graphene, which is one of the important methods to realize graphene modification [24–26]. Zhao *et al.* used first-principles calculation method to study the photoelectronic properties of P and Al co-doped graphene, and pointed out that the band gap of P–Al co-doped intrinsic graphene reached 0.45 eV [27]. Rezvan *et al.* investigated the borazine-doped nanographene material using halide as an anode material for lithium-ion batteries using first-principles calculations. Xinghua Zhu, Kun Liu, and other researchers studied the characteristics of graphene utilizing graphene to examine the impact of oxygen atom doping and adsorption [28]. It has been found that for opening the band gap of graphene, the adsorption of multiple oxygen atoms plays a huge role. Meanwhile, oxygen atoms, after doping into graphene, can repair the defects of filling graphene to a certain extent [29]. According to the above studies, we can find that doped graphene has better properties than intrinsic graphene and they can be used in a wide range of other fields.

Atomic doping provides an effective way to open the band gap of graphene for electronic devices such as field-effect transistors. Therefore, atomic doping can enrich the application of graphene in the field of field effect tubes. There are two types of FETs, namely p-type FETs and n-type FETs. The p-type field-effect tube uses a p-type semiconductor material, which is a semiconductor dominated by positively charged holes. The atomic size of boron atom is close to that of carbon (C) atom and has the ability to gain electrons by contributing holes. Therefore, boron-doped graphene shows potential applications in p-type semiconductor electronics [30]. The substitution of boron atoms for C atoms decreases the electron density of the substitution sites, while increasing the electron density of the adjacent C atoms. Several research groups have observed the properties of p-type semiconductors based on boron-doped graphene. Several research groups have observed the properties of p-type semiconductors based on boron-doped graphene. For example, Liu's group investigated the performance of p-type FETs fabricated with boron-doped graphene as a monolayer device, and the FETs possessed high carrier mobility [31].

The free concentration is much larger than the hole concentration in the impurity semiconductor. Nitrogen atoms can contribute their lone pair of electrons to the graphene network and are considered to be effective atoms for generating n-type semiconductor graphene channels. Theoretical studies have shown that the band gap of nitrogen-doped graphene reaches about 0.21 eV. P atoms can also give a pair of electrons, and their electron-giving ability is even much stronger than that of nitrogen atoms [32]. According to the results of Lee *et al.*, phosphorus doped graphene will produce stronger semiconductor behavior than nitrogen doping. Further studies show that the Dirac point of the material changes as the content of doped atoms increases, and the material will show more pronounced n-type semiconductor properties [33].

Therefore, according to the current research status of using doping atoms to change the electrical properties of graphene, it is believed that doping with P and Ga and P–Ga co-doping make graphene into n-type and p-type semiconductors with richer and better improvements in electrical and optical properties, thus broadening the scope and field of application of graphene materials.

Based on the above advances in graphene research, we have studied and compared the optoelectronic properties of P-doped graphene, (Ga)-doped graphene, and P–Ga co-doped graphene based on density functional theory. It provides some basic theoretical contribution to the improvement of graphene and its impact in band gap engineering applications is further strengthened, such as in sensors, new energy battery, nano electronic devices, super capacitor, *etc*.

2 Computation methods and models

2.1 Computational methods

Based on the framework of density flood theory, the microscopic properties of intrinsic graphene, P-doped graphene, Ga-doped graphene, and P–Ga co-doped graphene are calculated and analyzed using a first-principles approach for all models. Among these energy calculation modules

available, the plane wave (PW) and Cambridge series total energy package modules are more suitable for simulation of research targets. The exchange-correlation function we choose is from the generalized parsimonious gradient method developed by Perdew and Wang *et al.* It is a method that can accommodate both nonlinear objective functions and nonlinear constraints [34]. When calculating the graphene model parameters, in order to ensure that the model can be in a stable state, 410 eV was set as the PW cutoff energy and $5 \times 5 \times 1$ Å^{-1} as the k-point sampling density. In the geometric optimization of graphene, the convergence tolerance is set to 5.0×10^{-4} Å and the self-consistent field is set to 2.0×10^{-6} eV atom^{-1}, the maximum force and maximum stress were set at 0.03 eV Å^{-1} and 0.05 GPa, respectively.

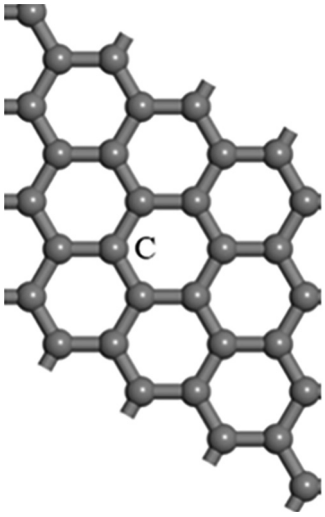

Figure 1: Intrinsic graphene model ($4 \times 4 \times 1$).

2.2 Computation models

A model-optimized graphene model is used as the simulation model of graphene. The molecular formula of graphene is C. Its single-layer atomic ring structure has hexagonal structural properties, which is a stable and symmetric structure. A covalent molecule is formed because each C is attached to three other adjacent C atoms, forming a solid chemical bond as well as a molecular structure. After completing the construction of the metacell, a larger scale system needs to be constructed in order to make the calculation results more accurate. Considering that as the system scales up, its computational volume also increases geometrically, in order to balance the computational volume and accuracy, the $4 \times 4 \times 1$ supercell model is built to describe graphene, which is shown in detail in Figure 1.

3 Results and discussion

3.1 Geometrical structures

Figure 2 shows the optimized models of the structures of P-doped graphene and Ga-doped graphene. In the optimized model, the bond length of C–P bond in P-doped graphene is 1.62 Å, which is similar to the bond length of C–C bond in intrinsic graphene (1.42 Å), which indicates that some properties of the molecular structure of doped graphene will be similar to that of intrinsic graphene. However, in the Ga-doped graphene model, the bond length of the C–Ga bond is longer than the C–C bond length in the intrinsic graphene with a bond length value of 1.75 Å due to the larger atomic radius of the Ga atom. Besides, Figure 3 shows the structure optimization model of P–Ga co-doped graphene. Due to the special structure of graphene, the relative positions of P and Ga atoms can be doped into different C atoms in graphene, *i.e.*, the anode position, the meta-pole position, and the para-pole position (Figure 3a–c). After analyzing and comparing these models, we concluded that the co-doping model with P and Ga in ortho-positions is the most stable.

In Table 1, it is clear that the C–P bonds (C3–P and C4–P) have the shortest bond length of 1.64 Å, followed by the C–Ga bond at 1.72 Å, and the P–Ga bond has the longest bond length of 1.95 Å. Therefore, for different doping, the bond length of graphene changes, which leads to a change in its properties.

Table 1 shows us very visually the bond lengths between the P and Ga atoms doped into graphene *in situ*.

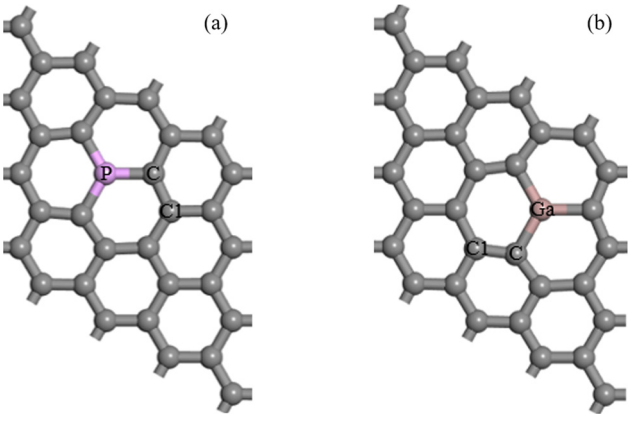

Figure 2: P-doped (a) and Ga-doped (b) graphene model.

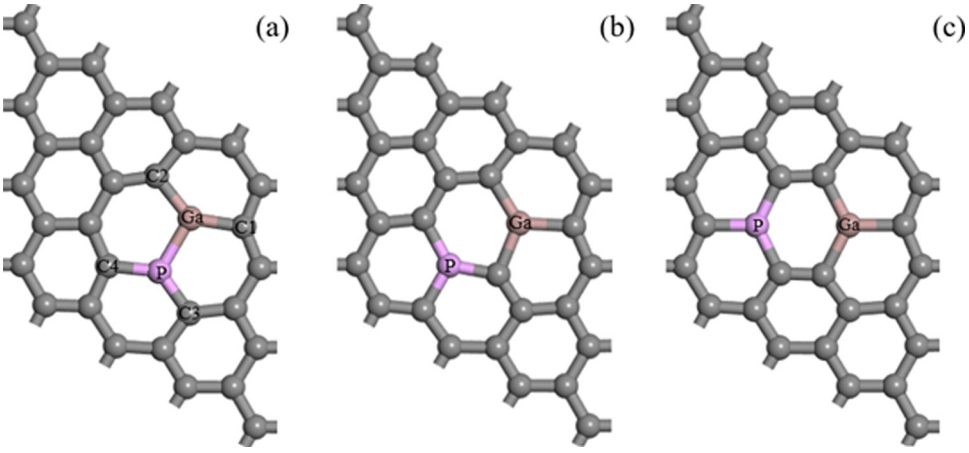

Figure 3: Three models of P–Ga co-doped graphene in different positions. (a) ortho; (b) meta and (c) para position.

Table 1: Bond lengths between atoms of P–Ga co-doped graphene

Bond types	Bond lengths (Å)
C1–Ga	1.72
C2–Ga	1.72
C3–P	1.64
C4–P	1.64
P–Ga	1.95

The bond length of the covalent bond formed by the Ga atom and the C atom directly connected to it is 1.72 Å. In addition, the bond length of the covalent bond between the P atom and the C atom directly connected to it is 1.64 Å. It is more obvious that the maximum chemical bond length of the P–Ga bond is 1.95 Å. The bond length between individual atoms in the P–Ga co-doped graphene is different from that of the intrinsic graphene. Based on these data, it can be judged that the molecular structure of P–Ga co-doped graphene is changed compared to the intrinsic graphene, and its properties are changed at the same time.

3.2 Electronic structures

Figure 4 shows the energy band diagrams with respect to intrinsic graphene, P-doped graphene, Ga-doped graphene, and P–Ga co-doped graphene. Through the study, the top of the valence band and the bottom of the conduction band of the intrinsic graphene model intersect at the K point in the Brillouin zone. The energy difference between the valence band top and conduction band

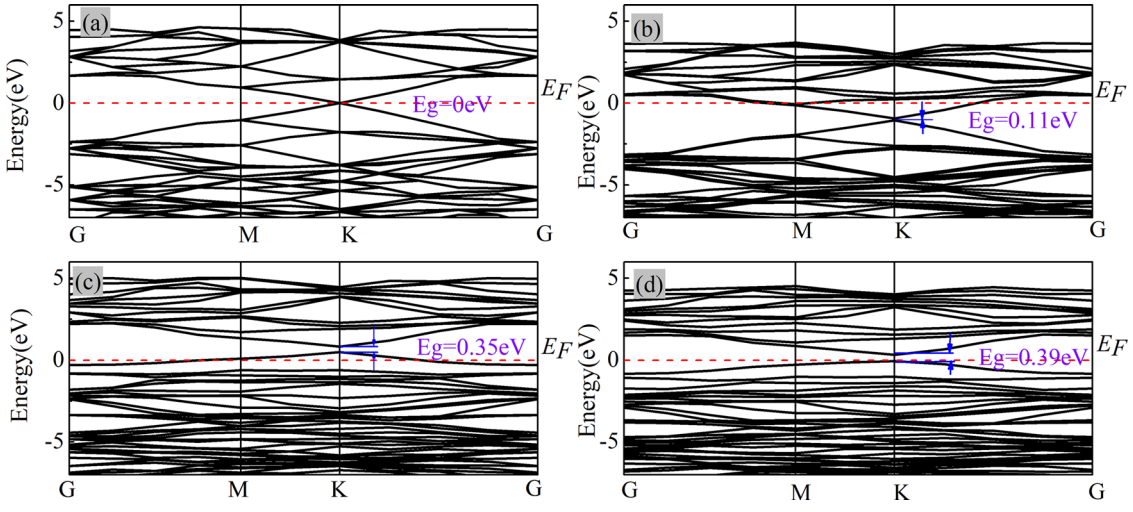

Figure 4: Band structures of (a) intrinsic, (b) P-doped, (c) Ga-doped, and (d) P–Ga co-doped graphene.

bottom is zero, *i.e.*, the forbidden band width is zero, and these can be seen in Figure 4a. This indicates that graphene is a material with zero forbidden band width and has excellent conducting properties. The doping of graphene with P atoms results in a jump of the electronic energy level to the lower energy region. At the same time, the Fermi energy level enters the conduction band (Figure 4b), resulting in the expansion of the forbidden band width to 0.11 eV.

After graphene is doped with Ga atoms, the electronic energy level jumps to the higher energy region. At the same time, it makes the Fermi energy level jump into the valence band (Figure 4c). This eventually allows the band gap to expand to 0.35 eV. When P–Ga is co-doped, the band gap of graphene is expanded to a maximum of 0.39 eV due to the combined effect of P and Ga atoms (Figure 4d). So based on the calculations and studies, it is found that doping plays a role in the expansion of the forbidden band width, and this result is important for improving the application of graphene as a semiconductor material.

We can conclude that the formation energy is an important factor to determine the system stabilization in the total energy of model systems. To further verify the stability of doped graphene systems, the formation energy was calculated for each system using the following equation:

$$E_{\text{formation}} = E_{\text{system}} - E_{\text{graphene}} + m\mu_{\text{carbon}} - n\mu_{\text{dopant}},$$

where E_{system}, E_{graphene}, μ_{carbon}, and μ_{dopant} stand for the total energy of doped graphene systems, pure graphene, the chemical potentials of C, and impurity atom, respectively. The doped graphene system can be synthesized by experimental methods, and we calculated and obtained the formation energy of the P–Ga co-doped graphene model for the adjacent, inter-, and para-site as $E_{\text{ortho}} = -8.273$ eV, $E_{\text{meta}} = -9.032$ eV, and $E_{\text{para}} = -8.865$ eV, respectively.

We can observe the electron density curves of intrinsic graphene, Ga-doped graphene, P-doped graphene, and P–Ga co-doped graphene in Figure 5. Regarding intrinsic graphene, the 2s and 2p orbitals of C are the main providers of its electrons and they contribute to the electron density. As the energy becomes stronger, the charges of 2p orbitals gradually dominate and play the main contribution. The doping of P atoms in graphene shifts the DOS curve to the lower energy region, leading to energy level migration in the conduction band of the Fermi energy

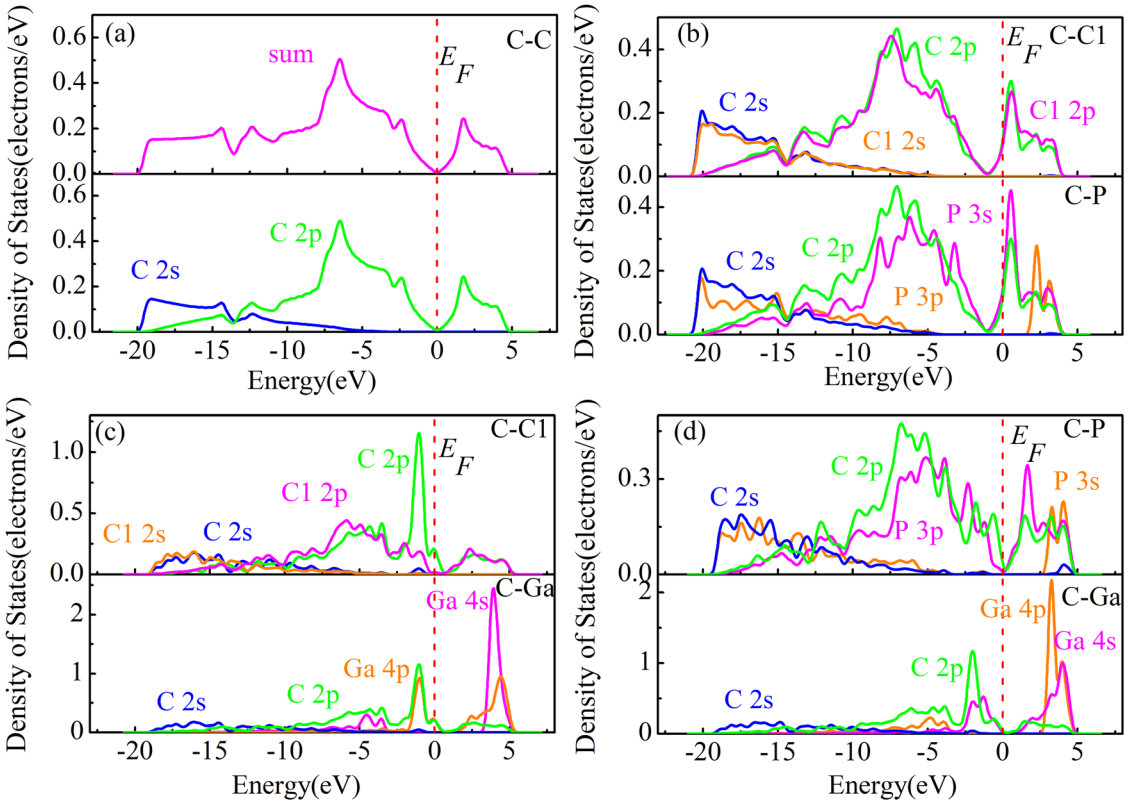

Figure 5: Density of states (DOS) of (a) intrinsic, (b) P-doped, (c) Ga-doped and (d) P–Ga co-doped graphene.

level. And compared with the C–C bond, the electron density of the C–P bond increases significantly in the energy range of –10 to –5 eV, and it is the electrons in the 3s and 3p orbitals of the P atom that play the main role in providing energy. In the same case, in Ga-doped graphene, the DOS curve of graphene increases due to the doping of Ga atoms, which in turn shifts the Fermi energy level in the valence band direction (Figure 5c). The potentials of both the conduction band energy level and the valence band energy level move upward, and the conduction band moves farther than the valence band energy level, so that the graphene band gap is widened in the range of 0.49–0.84 eV, with an expanded band gap width of 0.35 eV. While in the range of –10 to 5 eV, comparing the DOS curves of P–Ga co-doped graphene (Figure 5d) with those of Ga-doped graphene and P-doped graphene with each other, we can find from them that their curves are very different. Among them, the band gap of P–Ga co-doped graphene (0.39 eV) is larger than that of nitrogen-doped graphene and Ga-doped graphene. The main reason is that the C–P bonding of P–Ga co-doped graphene converts to high energy, while the C–Ga bonding of P–Ga co-doped graphene converts to low energy compared to P-doped graphene and Ga-doped graphene, respectively.

In Figure 6, the blue and red parts indicate the low and high electron numbers, respectively. When P atoms are doped into graphene, in graphene, some of the electrons on the hybridized orbitals of P atoms are trapped in the hybridized orbitals of C atoms, while the electron density around the P atoms is reduced (Figure 6b). In contrast to the previous, doping Ga atoms into graphene, a decrease in electron density around Ga atoms was observed. However, the increase in the electron density around the C atoms in graphene is evident. It shows that electrons are transferred from the orbitals of Ga atoms to those of C atoms (Figure 6c). In P–Ga co-doped graphene, the electrons around the P atoms and those around the Ga atoms are transferred to the C atoms. Furthermore, more electrons were transferred from Ga to C than from P to C. We can further analyze the above conclusions using the Mulliken population analysis (Table 2).

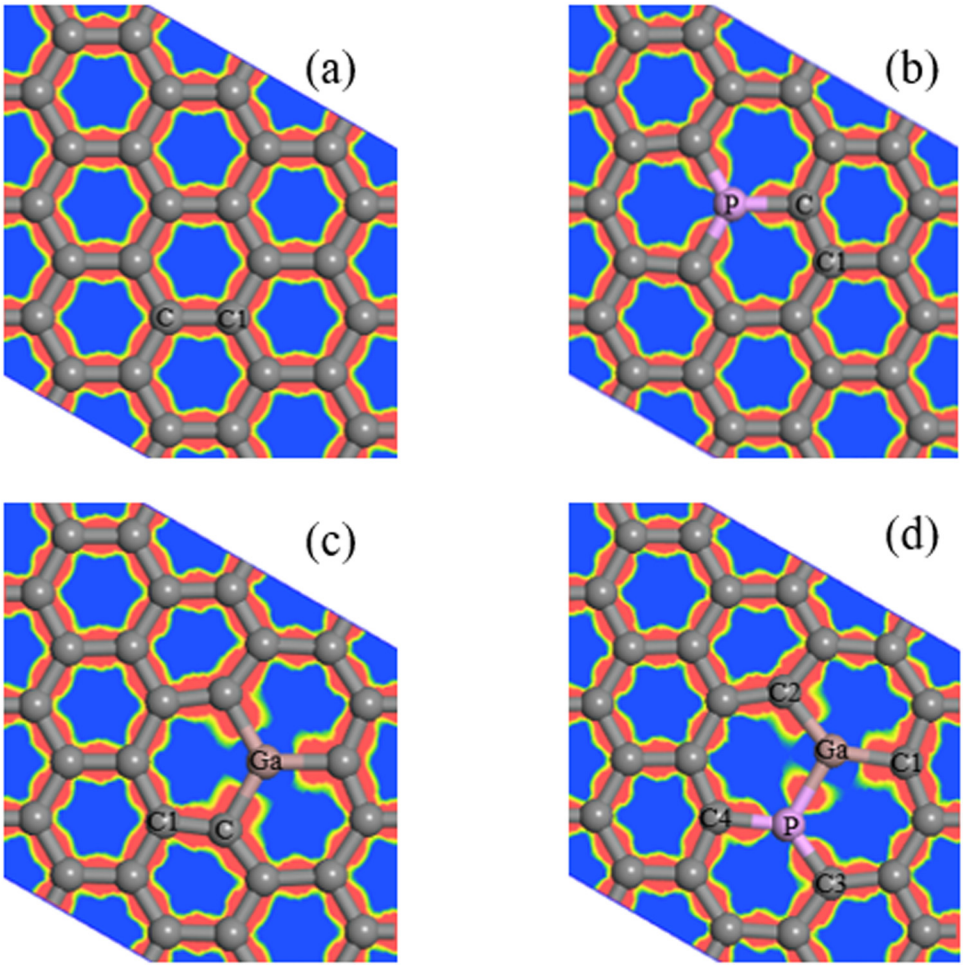

Figure 6: Electron density of (a) intrinsic graphene, (b) P-doped, (c) Ga-doped, and (d) P–Ga co-doped graphene.

Table 2: Mulliken charge populations of various doped graphene

Types of doping	Species	s	p	Charge (e)
Pure	C	1.05	2.95	0
P	C	1.14	3.27	−0.41
	P	1.07	2.53	1.40
Ga	C	1.18	3.29	−0.47
	Ga	0.65	0.60	1.75
P–Ga	C1 (C2)	1.17	3.31	−0.48
	C3 (C4)	1.15	3.21	−0.36
	P	1.31	3.08	0.61
	Ga	0.68	0.83	1.49

The electron gain and loss per C atom when doped in many different cases is shown in Table 2. In P-doped graphene, the P atom's hybridization orbital loses electrons and the C atom gains electrons. In the Ga-doped graphene, the C atoms gain electrons in the hybridization orbitals and the Ga atoms lose electrons. Besides, in the P–Ga co-doped graphene, the electrons lost by the Ga atoms are more than those lost by the P atoms in the P-doped graphene. From this, we can conclude that some electrons around the Ga atom are transferred to the hybridized orbitals of the C atom after doping. The electron density distribution of the graphene model with different doping systems shown in Figure 6 is consistent with these findings.

The electronegativities of Ga, C, and P atoms are 1.80, 2.55, and 2.19, respectively. The order of the electronegativities of these three atoms in these doping systems is C > P > Ga, Ga-doped graphene loses more electrons than P-doped graphene. Moreover, the electronegativity of C is greater than that of Ga, leading to the fact that in P–Ga co-doped graphene, the C atoms attached to Ga gain more electrons than the C atoms attached to P.

3.3 Optical properties

Figure 7 shows the complex refractive index of the graphene model doped with different atoms. In the Figure, (n) represents the real part of the complex refractive index indicating the dispersion of the medium to the

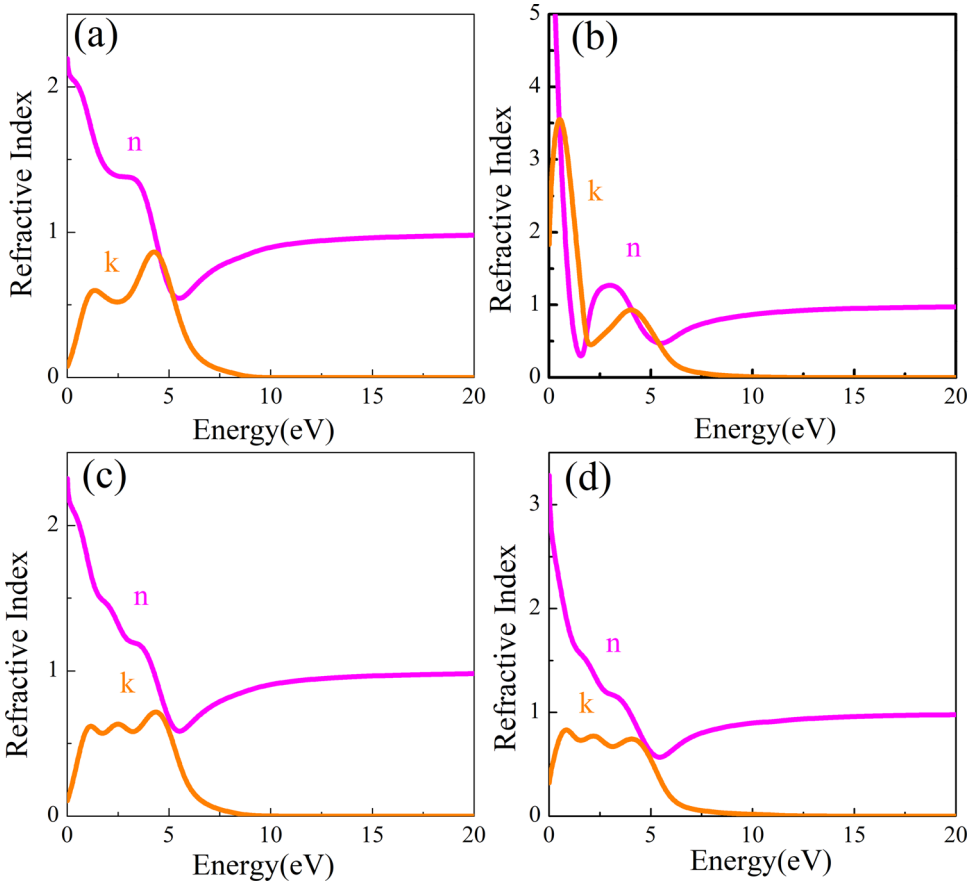

Figure 7: Complex refractive index curves of (a) intrinsic graphene, (b) P-doped, (c) Ga-doped, and (d) P–Ga co-doped graphene.

electromagnetic wave, and (k) is the imaginary extinction coefficient of the complex refractive index, indicating the absorption of the medium to the electromagnetic wave. The calculation of the complex refractive index N can be expressed by the following equation.

$$N = n + ki, \tag{1}$$

From the curves in Figure 7, we can find that the extinction coefficient k of intrinsic graphene has two different peaks from 0 to 5 eV, while its refractive index has a sharp peak and a gentle peak. Its refractive index peaks are 0.22 and 1.38, and its extinction coefficient peaks are 0.60 and 0.86. Compared with the intrinsic graphene, both n and k of the P-doped graphene are converted to lower energy states, with n decreasing more significantly and rapidly between 0 and 2.5 and the low-frequency peaks of n and k shifting upward. Graphene doped with Ga atoms, n and k also have relatively sharp differences from intrinsic graphene. The refractive index of light has only one peak and tends to decrease, the extinction coefficient appears as three high frequency peaks with little fluctuation in the Figure, and the high-frequency peaks become wider relative to the intrinsic graphene, but less intense than the intrinsic graphene. P–Ga co-doped graphene has some similarities with Ga-doped graphene, but its intensity is relatively small, k shifts slightly to the lower energy region, and the extinction coefficient changes in a flat trend.

With Figure 8, we can see the light absorption curves of doped graphene doped with different atoms. Where the light absorption coefficient η and extinction coefficient k have the following relationship:

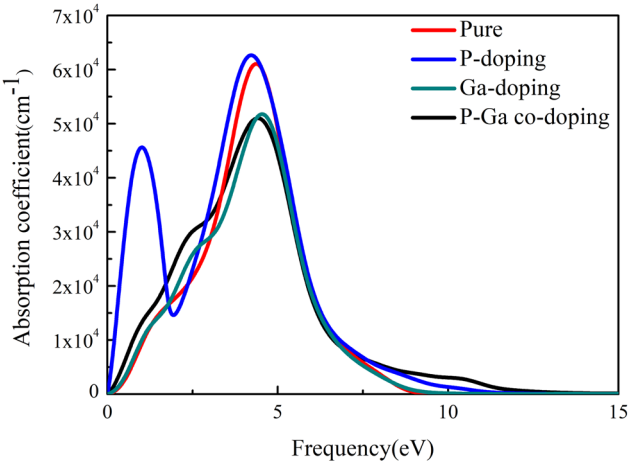

Figure 8: Optical absorption in intrinsic graphene and for different doping types of graphene.

$$\eta = \frac{2k\omega}{c}, \tag{2}$$

where ω is the frequency and c is the speed of light. The relationship between the coefficients of this equation leads to the fact that the absorption coefficient of light is proportional to the frequency. From Figure 8, we can see that the peak light absorption coefficient of graphene in the doped system has a certain degree of decline, especially the P–Ga co-doped graphene, which has the smallest light absorption coefficient among the four groups.

4 Conclusion

The electrical and optical properties of intrinsic graphene, P-doped graphene, Ga-doped graphene, and P–Ga co-doped graphene were calculated and studied in microscopic aspects based on the First-principles calculations. The intrinsic graphene is an excellent zero-bandgap semiconductor material, and the monolayer graphene has a unique linear energy band structure, which makes it have ultra-broadband saturable absorption properties and strong absorption capacity in the short-wave band. The unique energy band characteristics of graphene, in turn, limit its application in the field of nanoelectronic devices. The band gaps achieve was 0.11, 0.35, and 0.39 eV after the graphene was doped with P, Ga, and P–Ga, respectively. Therefore, it can be concluded that there is a significant improvement in the semiconductor properties after graphene doping. So for the study of graphene electronic devices, the advantages of doping P and Ga for bandgap broadening lie in the practical use in electronic devices, mainly focusing on graphene FETs. Especially in the case where transistors with good on/off ratios are required.

For P-doped graphene, electrons leave the hybridization orbital of the P atom and are gained by the C atom, with C gaining more electrons in its 3p orbitals and less in its 3s orbitals. In contrast, for Ga-doped graphene, the C atoms trap the electrons leaving the Ga atoms. For P–Ga doped graphene, a completely different electron gain/loss situation occurs than before, and when P and Ga atoms are co-doped with graphene, at this point, Ga atoms will lose more electrons within the P–Ga co-doped graphene than within the Ga-doped graphene, and P of P–Ga co-doped graphene will lose more electrons than P within the P-doped graphene. Compared with intrinsic graphene, the dispersion and extinction coefficients of P-doped graphene are converted to lower energy states, and the dispersion to electromagnetic waves decreases

more significantly and rapidly between 0 and 2.5, with the low-frequency peaks of the dispersion and extinction coefficients shifting upward. The dispersion and extinction coefficients of graphene doped with Ga atoms also differ relatively sharply from those of intrinsic graphene. The refractive index of light has only one peak and tends to decrease, and the extinction coefficient shows three high-frequency peaks with little fluctuation in the Figure, and the high-frequency peaks become wider relative to the intrinsic graphene. The optical absorption peaks are weaker and more pronounced for P–Ga doped graphene at low frequency conditions. These results indicate that there is great potential for practical applications and research of modified and doped graphene in the field of optoelectronic devices, for example, innovations and applications in solar cells, sensors, nanoelectronic devices, *etc*.

Acknowledgments: Y.W. thanks the High Performance Computing Center of Harbin Institute of Technology for calculation resource.

Funding information: Support by the Heilongjiang Excellent Youth Fund Project (YQ2019A004), and Scientific Research Project of Jinhua Advanced Research Institute (G202202).

Author contributions: All authors have accepted responsibility for the entire content of this manuscript and approved its submission.

Conflict of interest: The authors state no conflict of interest.

References

[1] Cai X, Han X, Zhao C, Niu C, Jia Y. Tellurene: an elemental 2d monolayer material beyond its bulk phases without van der Waals layered structures. J Semicond. 2020;41(8):1674–4926.
[2] Fu M, Zhu Z, Chen W, Yu H, Liu Q. Microwave-assisted synthesis of MoS_2/graphene composites for supercapacitors. J Mater Sci. 2020;55(34):16385–93.
[3] Chronopoulos DD, Medve M, Potsi G, Tomanec O, Scheibe M, Otyepka M. Tunable one-step double functionalization of graphene based on fluorographene chemistry. Chem Commun. 2020;56(13):1936–9.
[4] Wirth-Lima AJ, Alves-Sousa PP, Bezerra-Fraga W. Graphene's photonic and optoelectronic properties – A review. Chin Phys B. 2020;29(3):1674-1056.
[5] Novoselov KS, Fal'Ko VI, Colombo L, Gellert PR, Schwab MG, Kim K. A roadmap for graphene. Nature. 2012;490(7419):192–200.
[6] Young RJ, Kinloch IA, Gong L, Novoselov KS. The mechanics of graphene nanocomposites: A review. Compos Sci Technol. 2012;72(12):1459–76.
[7] Cao K, Feng S, Han Y, Gao L, Hue Ly T, Xu Z, et al. Elastic straining of free-standing monolayer graphene. Nat Commun. 2020;11(1):1–7.
[8] Chandra Y, Mukhopadhyay T, Adhikari S, Figiel L. Size-dependent dynamic characteristics of graphene based multi-layer nano hetero-structures. Nanotechnology. 2020;31(14):1361–6528.
[9] Sun Z, Liu Z, Li J, Tai GA, Lau SP, Yan F. Infrared photodetectors based on CVD-grown graphene and PbS quantum dots with ultrahigh responsivity. Adv Mater. 2012;24(43):5878–83.
[10] Chen Y, Yue YY, Wang SR, Zhang N, Feng J, Sun H. Graphene as a transparent and conductive electrode for organic optoelectronic devices. Adv Electron Mater. 2019;5(10):1–29.
[11] Liu Z, Chen Z, Wang C, Wang HI, Wuttke M, Wang XY, et al. Bottom-Up, on-surface-synthesized armchair graphene nanoribbons for ultra-high-power micro-supercapacitors. J Am Chem Soc. 2020;142(42):17881–6.
[12] Lee C-C, Suzuki S, Xie W, Schibli TR. Broadband graphene electro-optic modulators with sub-wavelength thickness. Opt Exp. 2012;20(5):5264–9.
[13] Han X, Zhang Z, Chen H, Zhang Q, Chen S, Yang Y. On the interface design of Si and multilayer graphene for a high-performance Li-ion battery anode. ACS Appl Mater Interfaces. 2020;12(40):44840–9.
[14] Sun F, Hu Z, Wu L, Chen J, Luo J, Wu X, et al. Reduced graphene oxide wrapped ultra-thin silicon nanowires for lithium ion battery anodes. J Phys Conf Ser. 2020;1520(1):1742–6596.
[15] Han J, Guo X, Ito Y, Liu P, Hojo D, Aida T, et al. Effect of chemical doping on cathodic performance of bicontinuous nanoporous graphene for Li-O_2 batteries. Adv Energy Mater. 2016;6(3):1–9.
[16] Hassoun J, Bonaccorso F, Agostini M, Angelucci M, Betti MG, Cingolani R, et al. An advanced lithium-ion battery based on a graphene anode and a lithium iron phosphate cathode. Nano Lett. 2014;14(8):4901–6.
[17] Stoller MD, Park S, Zhu Y, An J, Ruoff RS. Graphene-based ultracapacitors. Nano Lett. 2008;8(10):3498–502. doi: 10.1021/nl802558y.
[18] Zhu Y, Murali S, Stoller MD, Ganesh KJ, Cai W, Ferreira PJ, et al. Carbon-based supercapacitors produced by activation of graphene. Science. 2011;332(6037):1537–41.
[19] Liu C, Yu Z, Neff D, Zhamu A, Jang BZ. Graphene-based supercapacitor with an ultrahigh energy density. Nano Lett. 2010;10(12):4863–8.
[20] Wang Y, Shi Z, Huang Y, Ma Y, Wang C, Chen M, et al. Supercapacitor devices based on graphene materials. J Phys Chem C. 2009;113(30):13103–7.
[21] Wu ZS, Zhou G, Yin LC, Ren W, Li F, Cheng HM. Graphene/metal oxide composite electrode materials for energy storage. Nano Energy. 2012;1(1):107–31.
[22] Schwierz F. Graphene transistors. Nat Nanotechnol. 2010;5(7):487–96.
[23] Eda G, Fanchini G, Chhowalla M. Large-area ultrathin films of reduced graphene oxide as a transparent and flexible electronic material. Nat Nanotechnol. 2008;3(5):270–4.
[24] Strobel C, Chavarin CA, Leszczynska B, Leszczynski S, Winkler F, Killge S, et al. Demonstration of a graphene-base heterojunction transistor with saturated output current. J Appl Phys. 2019;125(23):234501.

[25] Farjadian F, Abbaspour S, Sadatlu MAA, Mirkiani S, Ghasemi A, Hoseini-Ghahfarokhi M, et al. Recent developments in graphene and graphene oxide: properties, synthesis, and modifications: A review. Chem Sel. 2020;5(33):10200–19.
[26] Liu H, Liu Y, Zhu D. Chemical doping of graphene. J Mater Chem. 2011;21(10):3335–45.
[27] Yuan XB, Tian YL, Zhao XW, Yue WW, Hu GC, Ren JF. Spin polarization properties of benzene/graphene with transition metals as dopants: First principles calculations. Appl Surf Sci. 2018;439:1158–62.
[28] Laref A, Ahmed A, Bin-Omran S, Luo SJ. First-principle analysis of the electronic and optical properties of boron and nitrogen doped carbon mono-layer graphenes. Carbon N Y. 2015;81(1):179–92.
[29] Zhu X, Liu K, Lu Z, Xu Y, Qi S, Zhang G. Effect of oxygen atoms on graphene: Adsorption and doping. Physe Low-Dimensional Syst Nanostructures. 2020;117:117.
[30] Wang M, Ford M, Phan H, Coughlin J, Nguyen TQ, Bazan GC. Fluorine substitution influence on benzo[2,1,3]thiadiazole based polymers for field-effect transistor applications. Chem Commun. 2016;52:3207–10.
[31] Wang H, Zhou Y, Wu D, Liao L, Zhao S, Peng H, et al. Synthesis of Boron-doped graphene monolayers using the sole solid feedstock by chemical vapor deposition. Small. 2013;9:1316–20.
[32] Zhou X, Zhao CH, Wu GF, Chen JH, Li YQ. DFT study on the electronic structure and optical properties of N, Al, and N-Al doped graphene. Appl Surf Sci. 2018;115:9935–40.
[33] Some S, Kim J, Lee K, Kulkarni A, Yoon Y, Lee S, et al. Highly air-stable phosphorus-doped n-type graphene field-effect transistors. Adv Mater. 2012;24:5481–6.
[34] Kresse G, Furthmüller J. Efficiency of ab-initio total energy calculations for metals and semiconductors using a plane-wave basis set. Comput Mater Sci. 1996;6(1):15–50.